Energy, Exergy and Uncertainty Analyses of the Thermal Response Test for a Ground Heat Exchanger

M.H. Sharqawy[♣,a], E.M. Mokheimer [b], M.A. Habib [b], H.M. Badr [b], S.A. Said [b] and N.A. Al-Shayea [b]

[a] Mechanical Engineering Department, Massachusetts Institute of Technology
77 Massachusetts Ave., Cambridge, MA 02139, USA

[b] Mechanical Engineering Department, King Fahd University of Petroleum & Minerals
Dhahran 31261, Saudi Arabia

Abstract

This paper presents energy, exergy and uncertainty analyses for the thermal response test of a ground heat exchanger. In this study, a vertical U-shaped ground heat exchanger with 80 m depth and 20 cm borehole diameter is installed for the first time at the university premises in Saudi Arabia. A mobile thermal response apparatus is constructed and used to measure the performance of the ground heat exchanger. The thermal response test was carried out four times at different thermal loads from September 2007 to April 2008. The energy and exergy transports of these thermal response tests were analyzed using the experimental results obtained in this period. The analysis provides a better understanding of the overall performance of vertical ground heat exchangers, verifies the thermal response test results and improves the experimental set up.

Key words: Energy, Exergy, uncertainty analysis, Ground heat exchanger, Ground coupled heat pump

---

♣ Corresponding author, Tel.: +1-617-308-7214, Fax: +1-617-253-3484, E-mail: mhamed@mit.edu

Nomenclature

Symbol	Designation	Units
d	borehole diameter	m
C_p	specific heat of circulating fluid	J/kg K
I^o	rate of irreversibility	W
L	ground heat exchanger borehole depth	m
M	any measured variable	
m^o	circulating fluid mass flow rate	kg/s
Q	heat transfer rate	W
R	any result variable	
T	temperature	^{o}C
$T_1 - T_{11}$	temperature at different positions in Fig. 1	^{o}C
W_{pump}	pump electrical power consumption	W

Greek Symbols

ε	effectiveness
η_{II}	second law efficiency
ω	uncertainty

Subscript

0	dead state
Calib	calibration
DAS	data acquisition system
g	ground
H	heater
loss1	losses from the heating section
loss2	losses from the hydraulic section

1. Introduction

Geothermal energy (geo-exchange) systems have been receiving growing interest on a global basis. The utilization of such systems has broadened in many engineering applications and is now recognized as a cost effective standard for energy conservation. In geo-exchange systems, a ground heat exchanger (GHE) is used to exchange heat with the underground environment and to provide cooling and heating for an ever-increasing number of applications. Applications include space heating and cooling, water heating, crop drying, agricultural greenhouses, etc. In vertical U-shaped ground heat exchangers, heat is extracted from or rejected to the ground by means of buried pipes, through which a heat carrier fluid is circulated in a closed circuit. To size or simulate the performance of a GHE, the thermal properties of ground at the vicinity of the GHE must be estimated. Such properties have a great effect on the number of boreholes required for any geo-exchange system [1].

The thermal response test is an effective method for the determination of the ground thermal properties. In this test, a known thermal load is applied to the GHE and accurate measurements of the inlet and outlet temperatures of the circulating fluid are recorded. The thermal response test was first presented by Mogensen [2] with a stationary test facility. Afterward, the mobile thermal response test facility appeared in Sweden [3], Canada, USA [4], Germany [5], Norway, Netherlands, England, Turkey [6], and Korea [7]. In Saudi Arabia, there are no studies undertaken so far related to the geo-exchange systems and it is of interest to examine such systems in this environment. This is a starting point for a future development in the geothermal energy research. In order to carry out technical and economical feasibility studies of utilizing geo-exchange systems, it is required to evaluate the performance of such systems in a given site by conducting thermal response tests on an installed GHE.

To evaluate the performance of the GHE and to develop systematic approaches for improving the geo-exchange systems, it is important to understand the mechanisms that degrade energy in such resources. The energy analysis as well as the full exergy analysis helps to identify where inefficiencies occur and where the improvements should be done to the geo-exchange components. Exergy analysis has been applied to various types of heat exchange systems by a number of researchers [8–13]. However,

the studies on exergy analysis of the thermal response test of GHEs are relatively few in numbers.

The objective of this paper is to conduct energy, exergy and uncertainty analyses on the thermal response test of a vertical U-shaped GHE, which has been installed for the first time at the university level in Saudi Arabia. Conducting such analyses is to verify the experimental measurements and measure the thermal performance of the GHE during the test. Moreover, conducting uncertainty analysis on the experimental measurements is very important to prove the accuracy of the obtained results.

2. GHE Installation

The location chosen for the GHE installation was a house garden located at KFUPM campus (Dhahran, Saudi Arabia, Latitude 26^o 17.9' N and Longitude 50^o 9.3' E). Two vertical boreholes separated by 1 meter distance were drilled each of diameter d = 20 cm and depth L = 80 m. In the first borehole, a single U-shaped pipe was inserted and, subsequently, the annular space was grouted with a Bentonite-sand mixture. The pipes are of high density polyethylene (HDPE) material, 1 ¼ inches diameter and SDR 11. The second borehole was used as a monitoring borehole where six thermocouples of type T (Copper – Constantan) were mounted at depths of 0.1, 0.2, 0.3, 10, 30 and 50 m. in addition to a seventh thermocouple of the same type that was mounted 0.2 m above ground surface to measure the ambient temperature. After that, the monitoring borehole was grouted with the same drilling cut.

3. Experimental Apparatus

The equipment of the experimental apparatus is set up on a small single-axle trailer. The equipment consists of a 1 hp circulation pump, 3 water heater elements in the range of 5 kW, water supply/purge tank, water filter, well insulated pipes and valves. The apparatus has two flexible hoses on the exterior of the trailer to allow attachment of the two HDPE pipes which are protruding from the vertical GHE. The instrumentation equipment includes a flowmeter, three thermistor probes and watt transducers. Temperatures at the inlet and outlet of the GHE and at various depths of the monitoring borehole as well as the flow rate and power input to the heating elements and the pump

were recorded with a data logger type Fluke Hydra. Figure 1 shows a layout of the experimental apparatus connected to the GHE and the monitoring borehole with a set of thermocouples mounted at different depths.

Power supply to the experimental apparatus is provided by connecting an 110V AC power line to the main breaker box that is located on the side wall outside of the trailer. The breaker box handles the power requirements for all equipment and instrumentations in the test apparatus. The water circulation system is composed of a water storage tank, filter, a circulation pump, control valves and a flow meter. The water storage tank is capable of storing a maximum of 35 gallons of water and is used to fill the GHE pipes and to purge the system before the test starts. The inlet and outlet ports of the tank are connected to 1" ball valves (V1 and V2 in Fig. 1) while the third port is a drain port connected to a 1" globe valve (V7 in Fig. 1). The outlet pipe from the tank is connected to the suction port of a 1-hp, 110-Volts motor-pump unit (model number: DAVEY XF111SS/Y) while the inlet pipe is connected to a turbine flowmeter (Omega FTB 4607) with a flow range of 0.22 to 20 GPM and ±2% accuracy. The output signal of the flowmeter is hooked to a calibrated flow display (Omega DPF 701) mounted in an instrumentation panel. A bypass valve (V3 in Fig. 1) between the inlet and outlet pipes is used after the purging process to separate the tank from the system (by closing valves V1 and V2) and operate the system in a closed loop. A standard in-line water cartridge filter is in between the circulating pump and the heaters section.

The heating system of the apparatus consists of three in-line water heater elements that have a screw-in mount for 1" NPT connection. Two water heaters are rated at 1.5 kW and the third one is rated at 2.0 kW at 110 volts. Each heating element is mounted down-up to ensure a perfect water contact and no air gabs that may result in hot spots on the heater surface. There are two inlet and outlet valves (V5 and V6 in Fig. 1) before and after the heating section and a bypass valve (V7 in Fig. 1) to separate this section from the system in the purging process. The stainless steel pipes within the heating section are insulated using a Fiberglas material to reduce the heat loss to the ambient. The input power to the heaters and to the pump is measured using two watt transducers mounted in the instrumentation panel. The watt transducers for the pump and for the heaters are Flex-Core PC5-117C and Flex-Core PC5-115C respectively. They are calibrated to give a DC voltage from 0 to 10 Volts for input power from 0 to 2000 Watt

with ±0.5% accuracy of the full scale reading. The power transducers are connected to the data logger to record the power input with time.

The water temperature is measured at the inlet and outlet to the GHE pipes in addition to the inlet to the heating section (T1, T2, and T3 in Fig. 1). The temperature sensors are 4 ½" stainless steel Omega ON-410-PP series thermistor probes with 1/8" NPT fitting and ±0.1°C accuracy. Three digital display meters mounted in the instrumentation panel receive the signal from the thermistors probes and display the temperature. The digital display meters are Omega DP25-TH-A series with ±0.1°C accuracy and analog output boards connected to the data logger. In addition, several temperature measurements are taken using type-T thermocouples manufactured by Omega and connected to the data logger. The exterior exposed flexible hoses connecting the U-shaped pipes to the inlet and outlet ports of the test apparatus are insulated to reduce the heat loss to the ambient. This heat loss is due to the distance from the ground surface to the trailer hook-up connectors. Foam insulation of 1 1/2" diameter is placed around the exterior flexible hoses then a five inches round duct insulation is pulled around the foam insulation.

The watt transducers, digital displays and thermocouples' analog readings are recorded by the data logger. Each of the digital display signals is a DC voltage signal configured on an output scale of 0-10 volts for each measurement. As each signal is retrieved, it is stored inside the data logger's memory and then downloaded at a later time without losing any measurements.

4. Thermal Response Test

Before starting the thermal response test, the undisturbed ground temperature (T_g) is measured by connecting the U-shaped pipes to the thermal response test apparatus and water is circulated for approximately 60 minutes by the pump. The data logger is set to record the GHE inlet and outlet temperatures (T_2 and T_3 in Fig. 1) every 10 seconds and the electric heating elements are turned off. Figure 2 shows the inlet and outlet temperature variations with time. It is clear that after 30 to 40 minutes, the temperature fluctuations between T_2 and T_3 are evened out at the mean ground temperature. The undisturbed ground temperature is considered to be the one after the decay of the fluctuations in T_2 and T_3.

The thermal response test starts directly after the circulating fluid temperature reaches the undisturbed ground temperature by switching the heaters on and adjusting the pump flow rate such that a temperature difference of 3 to 4 ^{o}C is produced between the inlet and outlet section of the GHE. During the test, all temperatures, flow rate and power consumptions are recorded until the circulating fluid temperature attain a steady-state condition. This may take from 75 to 240 hours (10 days) depending on the thermal load and ground properties.

The thermal response test was carried out four times at different thermal loads from September 2007 to April 2008. The thermal loads tested were Q = 1.5, 2, 3 and 3.5 kW according to the nominal capacities of the electrical heaters installed in the test apparatus. In the following analysis, the thermal response test results for the 1.5 kW thermal load are presented and analyzed. The recorded inlet and outlet circulating fluid temperatures (T_2 and T_3) are shown in Fig. 3. As it is seen in this figure the inlet and outlet circulating fluid temperature increased continuously with time until a steady-state was reached. During the test, the volumetric flow rate of the pump remained nearly constant in a range between 0.105 and 0.117 with a mean value of 0.111 L/s. The mean electrical power input to the water heater is 1.43 kW while the mean electrical power input to the pump is 0.56 kW as shown in Fig. 4. It is important to note that the starting time in Figures 3 – 4 (t = 0) is at 10:05 AM and this test was conducted for 10 days.

As shown in Fig. 4, there is a periodical fluctuation in the input electrical power of the heaters and the pump. This fluctuation is due to the variations of the supply voltage from the electrical grid. The peaks of the input electrical power occur at night while the dips occur at noon because the load on the electrical grid is very high at noon and hence the supply voltage decreases. These small fluctuations in the input electrical power swing the inlet and outlet circulating fluid temperatures as shown in Fig. 3. However, these temperatures increase with time until approaching a steady-state condition.

On the other hand, the fluctuation in the pump input power creates small variations in the volume flow rate. It is important to note that the inlet circulating fluid temperature to the GHE (T_2) is very sensitive to the fluctuations in the input electrical power which is clearly shown in Fig. 3. This may be explained by the thermal dynamics of the

temperature near to the heaters outlet section which has a small response time. However, the outlet temperature from the GHE (T_3) has moderate fluctuations unlike T_2 because of the heat transfer processes occurring in the ground.

The direct measurements of the ground temperature in the monitoring borehole (which is 1 meter apart from the GHE borehole) are shown in Figures 5 and 6. In Fig. 5, the ground temperatures at depths of 10 m, 30 m and 50 m (T_9, T_{10} and T_{11}) are plotted with time during the thermal response test period. As shown in this figure, the ground temperature at 10 m depth does not change with time, while that at 30 and 50 meters depths increase slowly with time. The rate of increase of the ground temperature at 50 m depth is higher than that at 30 m as indicated in Fig. 5. From this result, the ground temperature is stable over the borehole depth of 10 m. However below 10 m, the groundwater and natural convection has an effect on the ground condition.

In Fig. 6, the ground temperature at depths of 0.1 m, 0.2 m and 0.3 m (T_6, T_7 and T_8) as well as the ambient temperature (T_5) are plotted against time during the thermal response test period. As shown in this figure, there is a periodical variation of these temperatures with daylight and nighttime except for day 7 (9^{th} April, 2008) since there was rain during that day. We notice from Fig. 6 that the ambient temperature reaches its maximum at noon and its minimum occurs at midnight. However, there is a temperature shift with time in the three values of the ground temperatures at 0.1, 0.2 and 0.3 m depths. At noon, the ground temperature T6 at 0.1 m is higher than the lower ones while at midnight the ground temperature T8 at 0.3 m is the highest. This means that there is heat gain from the atmosphere at daylight while there is heat loss at nighttime. Since there are many factors affecting the heat transfer from the ground surface including radiation, convection and evaporation, we can see the combined effect of all of these parameters in Fig. 6.

5. Energy and Exergy Analysis

A simple energy model proposed to account for heat exchange between the different parts of the system and the surrounding environment is shown schematically in Fig. 7. In this figure, the heating section starts at Point 1 and ends at Point 2 while the GHE section starts at Point 2 down to the ground and up to Point 3. The piping, pipe fittings

and pump namely the hydraulic section starts at Point 3 and ends at Point 1 to close the cycle. There is an electrical heating power input to the heating section, Q_H and electrical power input to the circulating pump, W_{pump}. In addition to the heat dissipated in the ground by the GHE, Q_{GHE}, heat losses from the heating section, Q_{loss1} and heat losses from the hydraulic section, Q_{loss2} are all considered in the analysis.

The energy analysis is based on the application of the first law of thermodynamics on each section, while the exergy analysis is essentially that of available energy analysis which is discussed in detail in many references [14]. The concepts of exergy destruction, irreversibility and lost work are essentially similar [15]. The following assumptions are adopted for the first and second law analyses.

1. At each time step, all processes are assumed to be steady with negligible potential and kinetic energy effects.
2. The directions of heat transfer to the system and work done by the system are positive.
3. Water pressure drops in the tubing connecting the components (excluding GHE pipes) are ignored, since their lengths are short.
4. The dead state of the water is taken at the average ambient temperature during the test (T_0 = T5)

Under the above mentioned assumptions for a general steady process, the energy and exergy balances are applied to find the actual heat transferred to the ground (Q_{GHE}), heat loss from the heating section (Q_{loss1}), heat loss from the hydraulic section (Q_{loss2}), the rate of irreversibility (I^o) and the GHE effectiveness (ε) and the exergy efficiency (η_{II}) [16, 17].

(a) First law analysis (Energy balance)

$$Q_{GHE} = m^o\, C_p \left(T_2 - T_3\right) \tag{1}$$

$$Q_{loss\,1} = Q_H - m^o\, C_p \left(T_2 - T_1\right) \tag{2}$$

$$Q_{loss2} = W_{pump} - m^o\, C_p \left(T_1 - T_3\right) \tag{3}$$

$$\%Q_{GHE} = \frac{Q_{GHE}}{Q_H + W_{pump}} \tag{4}$$

$$\%Q_{loss\,1} = \frac{Q_{loss\,1}}{Q_H + W_{pump}} \tag{5}$$

$$\%Q_{loss\,2} = \frac{Q_{loss\,2}}{Q_H + W_{pump}} \tag{6}$$

(b) Second law (Exergy) analysis

$$I^o = T_0 \left[m^o\, C_p \ln\left(\frac{T_3}{T_2}\right) + \frac{Q_{GHE}}{T_g} \right] \tag{7}$$

$$\eta_{II} = \frac{Q_{GHE}}{m^o\, C_p \left[\left(T_2 - T_3\right) + T_0 \ln\left(\frac{T_2}{T_3}\right) \right]} \tag{8}$$

$$\varepsilon = \frac{Q_{GHE}}{m^o\, C_p \left(T_2 - T_g\right)} \tag{9}$$

To verify that the test satisfies the first law of thermodynamics, the summation of the percentage heat transferred to the ground and the heat losses should be equal to 1. Figure 8, shows the actual heat transferred to the ground (Q_{GHE}) and the heat losses in the heating section (Q_{loss1}) and the hydraulic section (Q_{loss2}) as calculated by Eqs. 1 – 3 respectively. Even with provisions taken regarding thermal insulation of the hydraulic circuit, ambient coupling was observed in Fig. 9. This figure shows the percentage of these heat losses with respect to the total energy added to the system (Q_H and W_{pump}). As seen in Fig. 9 the average heat loss from the heating section is 5.1 % while the average heat loss from the hydraulic section is 14.9 %. The remaining part of energy (80%) is delivered to the GHE. It is worth mentioning that, this energy balance should be conducted in the ground thermal response test in order to calculate the actual heat transferred to the ground (Q_{GHE}). This amount of actual heat transfer (Q_{GHE}) should be taken in the GHE analysis to determine the ground thermal properties by using any of the well known analytical and numerical models [18 – 20]. Moreover, the heat flux rejected to the ground is calculated by dividing the actual heat transferred through the GHE (Q_{GHE} and not the input power to the heaters) over the surface area of the borehole.

To make sure that the experimental test satisfies the second law of thermodynamics, the calculated irreversibility of the GHE must be positive at all readings. This is the entropy increase principle which was first introduced by Lord Kelvin [16] for the real processes in any closed system. Figure 10 shows the rate of irreversibility for the GHE as calculated by Eq. (7) during the thermal response test. As indicated in this Figure, the rate of irreversibility is always positive and increases with time. It increases because the temperature difference between the system (circulating fluid of the GHE) and the surrounding (ground) increase with time. It is well known that, any heat transfer process becomes more and more irreversible as the temperature difference between the two bodies increases [16].

Another important parameter from the exergy analysis is the second law efficiency. This efficiency indicates how much idealization of the heat transfer process in the GHE. The value of the second law efficiency of the GHE (η_{II}) as calculated by Eq. (8) is constant with time and has a value of 51.1 %. This value is considered acceptable since in most heat exchangers (shell and tube, tube-in-tube, plate HX) the second law efficiency is in the range of 40% - 60% as provided by Hewitt et al. [21].

One last parameter which can be used to evaluate the operation of the GHE is the effectiveness. As any other heat exchanger, the effectiveness is the ratio between the actual rate of heat transfer to the maximum amount of heat rate that could be transferred. The maximum value of the heat rate that could be transferred to the ground may be calculated by replacing the outlet circulating fluid temperature (T3) with the minimum temperature that could be reached which is the undisturbed ground temperature (T_g). This definition is clearly written in Eq. (9). Figure 11 shows the calculated effectiveness of the GHE with time. As indicated in the figure, the effectiveness is equal to unity at the beginning of the test because the circulating fluid temperature is the same as the ground temperature at the test start up. The final steady value of the GHE effectiveness is 46.6 % which is considered as an acceptable value according to Hewitt et al. [21].

6. Uncertainty Analysis

It is well known that errors and uncertainties in any experiments can arise from instrument selection, instrument condition, instrument calibration, environmental conditions, observation and reading and test planning. Uncertainty analysis is needed to prove the accuracy of the experiments. The uncertainty analysis is performed using the method described by Holman [22]. In the present study, the temperatures, flow rates and electrical powers are measured with appropriate instruments as explained in section 3. Results are calculated from these measured parameters such as (Q_{GHE}), (Q_{loss1}), (Q_{loss2}), (I^o), (ε) and (η_{II}). The total uncertainty of any measured parameter may be calculated as follows,

$$\omega_M = \left[\omega_{sensor}^2 + \omega_{DAS}^2 + \omega_{Calib}^2\right]^{1/2} \tag{10}$$

where ω_M is the uncertainty in any measured parameter M, ω_{sensor} is the uncertainty in the sensor reading, ω_{DAS} is the uncertainty associated with the data acquisition system and ω_{Calib} is the uncertainty in the calibration procedure. The uncertainty of each measured variable (given in Table 1) is calculated using Eq. (10) and the data provided from the manufacturer. As shown in Table 1 (top part), the uncertainty in the temperature measurements using thermistors T1, T2 and T3 is 0.1 ^oC. While for the thermocouples T4 – T11, the uncertainty is 0.2 ^oC. These uncertainties include both the sensor and the data acquisition system uncertainties as provided by the manufacturer. The uncertainty in the measured flow rate is given in Table 1 by ±2.0 % and the uncertainty of the watt transducer is ±1. These uncertainties include sensor, data acquisition and calibration uncertainties as provided by the manufacturer.

The uncertainty arising in calculating any result (R) due to several independent variables uncertainties (ω_{M1}, ω_{M2} ... ω_{Mn}) is given by Coleman and Steele [23] and can be expressed as;

$$\omega_R = \left[\left(\frac{\partial R}{\partial M_1}\omega_{M_1}\right)^2 + \left(\frac{\partial R}{\partial M_2}\omega_{M_2}\right)^2 + \cdots + \left(\frac{\partial R}{\partial M_n}\omega_{M_n}\right)^2\right]^{1/2} \tag{11}$$

where the result R is given as a function of the independent variables M_1, M_2 ... M_n and (ω_{M1}, ω_{M2} ... ω_{Mn}) are the uncertainties in the independent variables. Equation (11) is a general equation that is used to calculate the uncertainty in each result. It is applied on Eq. (1), Eq. (2), Eq. (3), Eq. (7), Eq. (8) and Eq. (9) to calculate the uncertainty in Q_{GHE}, Q_{loss1}, Q_{loss2}, I^o, ε and η_{II} respectively. This has been done easily by using the uncertainty propagation function in Engineering Equation Solver software (EES) [24]. Total uncertainties of the measured and calculated parameters are presented in Table 1. As indicated in Table 1, the highest uncertainty occurs in the heat loss from the heating section (±9.58%) Q_{loss1}. However, the uncertainty occurs in the value of the second law efficiency is ±4%. The uncertainty of most concern is that associated with measurements of Q_H and Q_{pump}, which have a large impact on the error in the heat dissipated to the ground (Q_{GHE}). The uncertainty of Q_{GHE} calculated is 5.03% and it was found that this value did not change with the increase of heater power.

7. Concluding remarks

In this study, a vertical U-shaped ground heat exchanger with 80 m depth and 20 cm borehole diameter was installed at KFUPM, Dhahran, Saudi Arabia. A mobile thermal response test apparatus was constructed and used to measure the performance of the GHE. The experimental results of the thermal response test were evaluated using energy, exergy and uncertainty analyses. It was found that the experimental results satisfy both first and second laws. In addition, the GHE has a good thermal performance with an effectiveness of 46.6±3.5 % and a second law efficiency of 51.1±2 %. The analysis provides a better understanding to the overall performance of vertical GHE and verifies and improves the thermal response test experimental set up.

Acknowledgements

The authors acknowledge the support provided by King Abdulaziz City for Science and Technology (KACST) and King Fahd University of Petroleum and Mineral (KFUPM) for this research project. The experimental work was funded by KACST under project number AR-23-83.

References

[1] Florides G., Kalogirou S., Ground heat exchangers – A review of systems, models and applications. *Renewable Energy* 2007; 32 (15): 2461-2478.

[2] Mogensen P. Fluid to duct wall heat transfer in duct system heat storages. Proceedings of the International Conference on Subsurface Heat Storage in Theory and Practice, Stockholm, Sweden, June 6–8. 1983; 652 – 657.

[3] Eklof C., Gehlin S. TED – a mobile equipment for thermal response test. Master's thesis, Lulea University of Technology; Sweden, 1996.

[4] Austin WA. Development of an in-situ system for measuring ground thermal properties. Master's thesis. Stillwater, OK: Oklahoma State University; 1998.

[5] Sanner B, Reuss M, Mands E, Muller J. Thermal response test – experiences in Germany. Proceedings of Terrastock 2000, 8th International Conference on Thermal Energy Storage, Stuttgart, August 28th – September 1st, vol. 1. 2000; 177 – 182.

[6] Paksoy H, Gurbuz Z, Turgut B, Dikici D, Evliya H. Aquifer thermal storage (ATES) for air conditioning of a supermarket in Turkey. Proceedings of World Renewable Energy Congress-VII 2002, Cologne, Germany, 29 June –5 July. 2002.

[7] Kyoungbin L., Sanghoon L., Changhee L., An experimental study on the thermal performance of ground heat exchanger. *Experimental Thermal and Fluid Science* 2007; 31(8): 985 – 990.

[8] Bejan A., Fundamentals of exergy analysis, entropy generation minimization, and the generation of flow architecture, *International Journal of energy Research* 2002, 26 (7): 0 – 43.

[9] Ozgener L., Hepbasli A., Dincer I., Energy and exergy analysis of geothermal district heating systems: an application, *Building and Environment* 2005; 40 (10): 1309 – 1322.

[10] Ozgener L., Hepbasli A., Dincer I., Energy and exergy analysis of Salihli geothermal district heating system in Manisa, Turkey, *International Journal of energy Research* 2005, 29 (5): 393 – 408.

[11] Hepbasli A., Akdemir O., Energy and exergy analysis of a ground source (geothermal) heat pump system, *Energy Conversion and Management*, 2004; 45 (5): 737 – 753.

[12] Kara Y., Experimental performance evaluation of a closed-loop vertical ground source heat pump in the heating mode using energy analysis method, *International Journal of energy Research* 2007, 31 (15): 1504 – 1516.

[13] Kanoglu M., Dincer I., Rosen M.A., Understanding energy and exergy efficiencies for improved energy management in power plants, *Energy Policy*, 2007; 35(7): 3967 – 3978.

[14] Incropera F.P., Dewitt D.P., Fundamentals of heat and mass transfer, 5th edition, John Wiley & Sons Inc, NY, 2002

[15] Krakow K.I., Exergy analysis: Dead-state definition, *ASHRAE Transactions*, 1991; 97(1): 328 – 36.

[16] Cengel Y, Boles MA. Thermodynamics: An engineering approach. 4th Ed. McGraw-Hill, 2001.

[17] Bejan A. Advanced engineering thermodynamics. Wiley, 1988.

[18] Ingersoll L.R., Plass H.J., Theory of the ground pipe heat source for the heat pump, *Heating Piping & Air Conditioning*, 1948: 119 – 122.

[19] Deerman J.D., Kavanaugh S.P., Simulation of vertical U-tube ground coupled heat pump systems using the cylindrical heat source solution, *ASHRAE Transactions, 1991;* 97 (1): 287 – 295.

[20] Eskilson P., Claesson J., Simulation model for thermally interacting heat extraction boreholes, *Numerical Heat Transfer*, 1988; 13: 149 – 165.

[21] Hewitt G. F., Shires G. L., Bott T. R., Process Heat Transfer, CRC Press LLC, New York, 1994.

[22] Holman J. P., Experimental methods for engineers, 7th Ed. New York: McGraw-Hill, pp. 48–143. 2001.

[23] Coleman H. W., W. G. Steele, Experimentations and Uncertainty Analysis for Engineers, 2nd Ed., Wiley-Interscience, 1999.

[24] Klein, S.A., Alvarado, F.L., Engineering Equation Solver, Version 8.175. F-Chart Software, WI. 2008.

List of Figures

List of Tables

Table 1

Description	**Total Uncertainty**
Measured parameters	
Circulating fluid inlet temperature to the Heaters, T1	±0.1 (^{o}C)
Circulating fluid inlet temperature to the GHE, T2	±0.1 (^{o}C)
Circulating fluid outlet temperature from the GHE, T3	±0.1 (^{o}C)
Ambient and ground temperatures, T4 – T11	±0.2 (^{o}C)
Circulating fluid mass flow rate, m_w	±2.0 (%)
Electrical power inputs to the heaters and the pump, Q_H, W_{pump}	±1 % (of the full scale)
Calculated parameters	**Max. Total Relative Uncertainty**
Actual heat transfer rate to the ground, Q_{GHE}	±5.03 (%)
Heat loss from the heating section, Q_{loss1}	±9.58 (%)
Heat loss from the hydraulic section, Q_{loss2}	±5.07 (%)
Rate of Irreversibility in the GHE, I^{o}	±1.25 (%)
Second law efficiency, η_{II}	±4.00 (%)
GHE effectiveness, ε	±7.50 (%)

Fig. 1

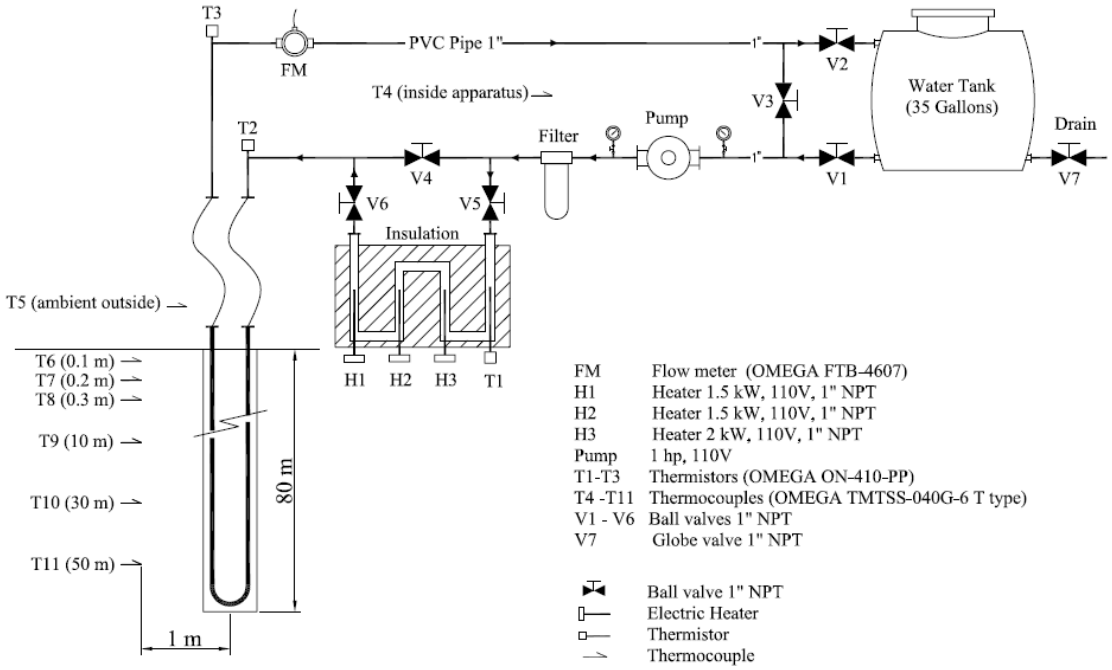
T3
FM
PVC Pipe 1"
V2
Water Tank
(35 Gallons)
T4 (inside apparatus)
V3
Pump
T2
Filter
Drain
V4
V1
V7
V6
V5
Insulation
T5 (ambient outside)
T6 (0.1 m)
T7 (0.2 m)
T8 (0.3 m)
T9 (10 m)
T10 (30 m)
T11 (50 m)
H1
H2
H3
T1
80 m
1 m
FM Flow meter (OMEGA FTB-4607)
H1 Heater 1.5 kW, 110V, 1" NPT
H2 Heater 1.5 kW, 110V, 1" NPT
H3 Heater 2 kW, 110V, 1" NPT
Pump 1 hp, 110V
T1-T3 Thermistors (OMEGA ON-410-PP)
T4 -T11 Thermocouples (OMEGA TMTSS-040G-6 T type)
V1 - V6 Ball valves 1" NPT
V7 Globe valve 1" NPT
Ball valve 1" NPT
Electric Heater
Thermistor
Thermocouple

Fig. 2

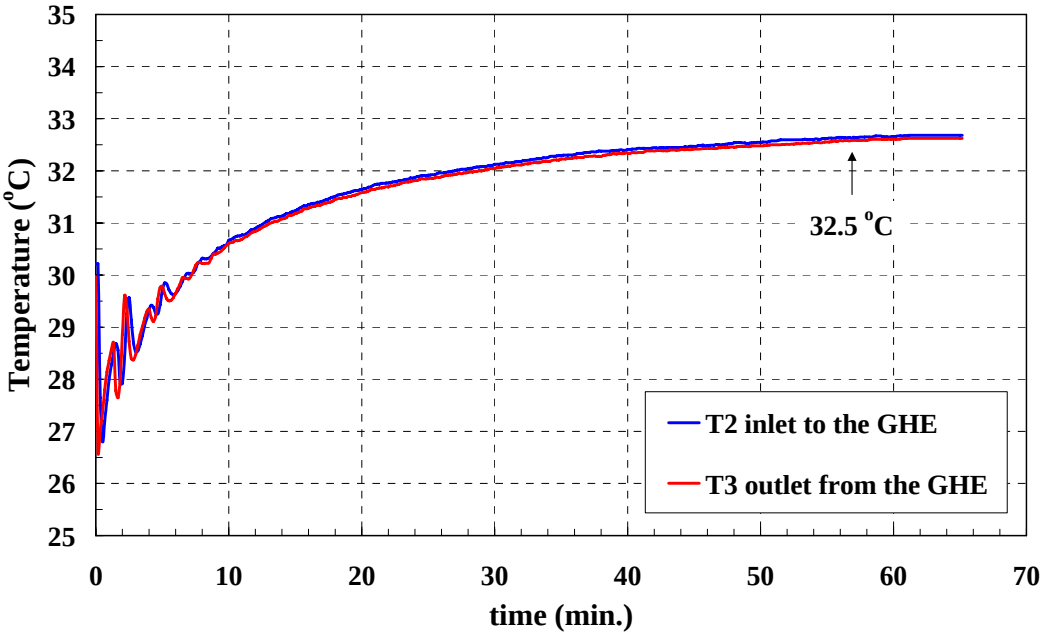
Temperature (°C)
time (min.)
32.5 °C
T2 inlet to the GHE
T3 outlet from the GHE
35
34
33
32
31
30
29
28
27
26
25
0
10
20
30
40
50
60
70

Fig. 3

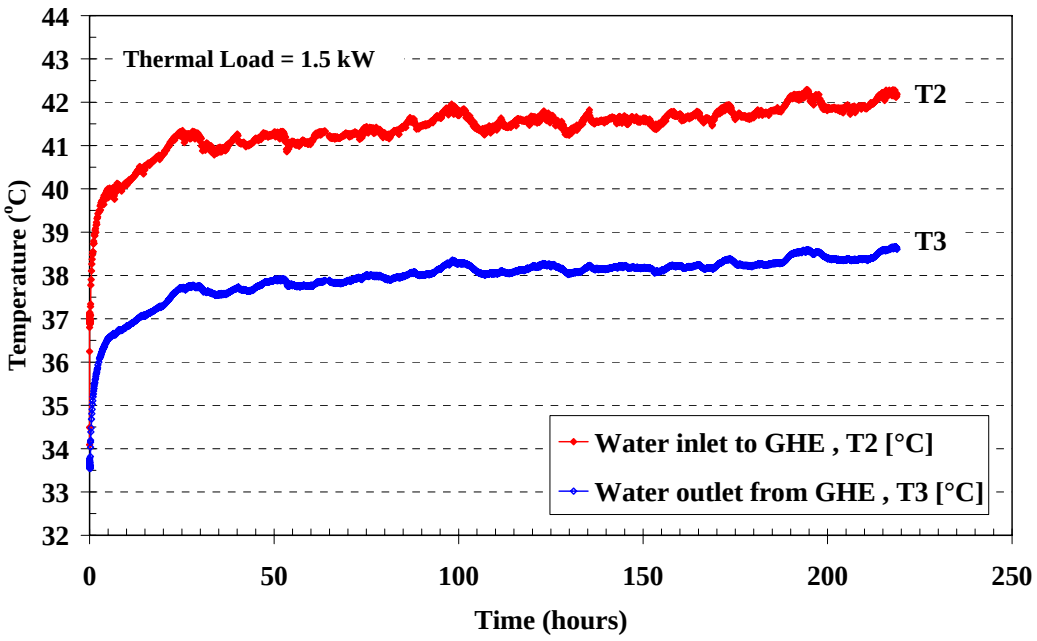
Thermal Load = 1.5 kW
T2
T3
Water inlet to GHE , T2 [°C]
Water outlet from GHE , T3 [°C]
Temperature (°C)
Time (hours)
44
43
42
41
40
39
38
37
36
35
34
33
32
0
50
100
150
200
250

Fig. 4

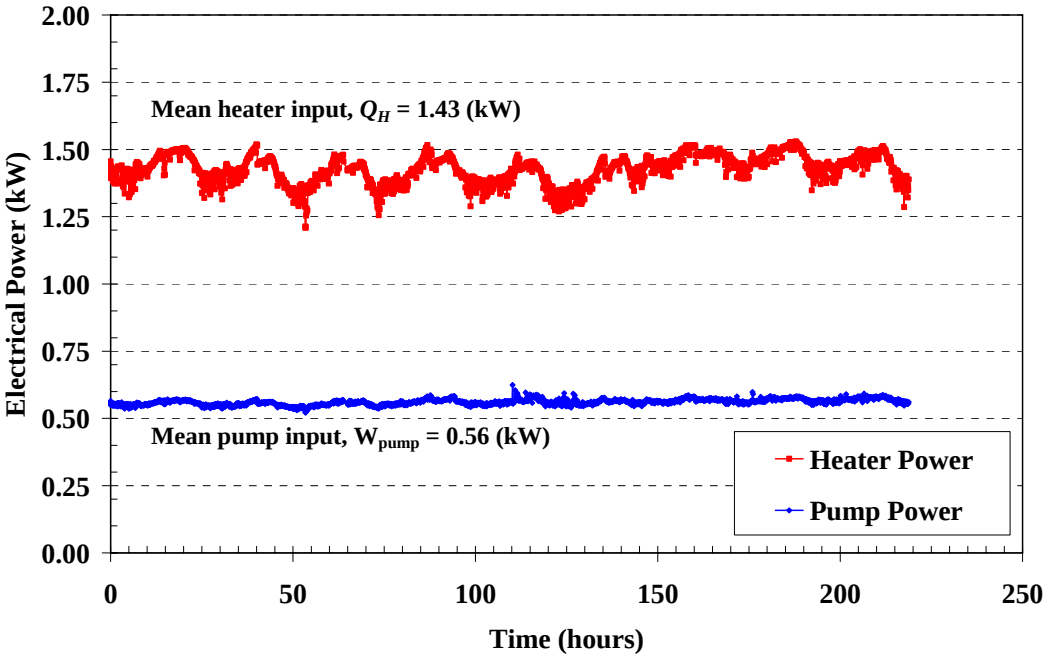
2.00
1.75
1.50
1.25
1.00
0.75
0.50
0.25
0.00
Electrical Power (kW)
Mean heater input, Q_H = 1.43 (kW)
Mean pump input, W_{pump} = 0.56 (kW)
Heater Power
Pump Power
0
50
100
150
200
250
Time (hours)

Fig. 5

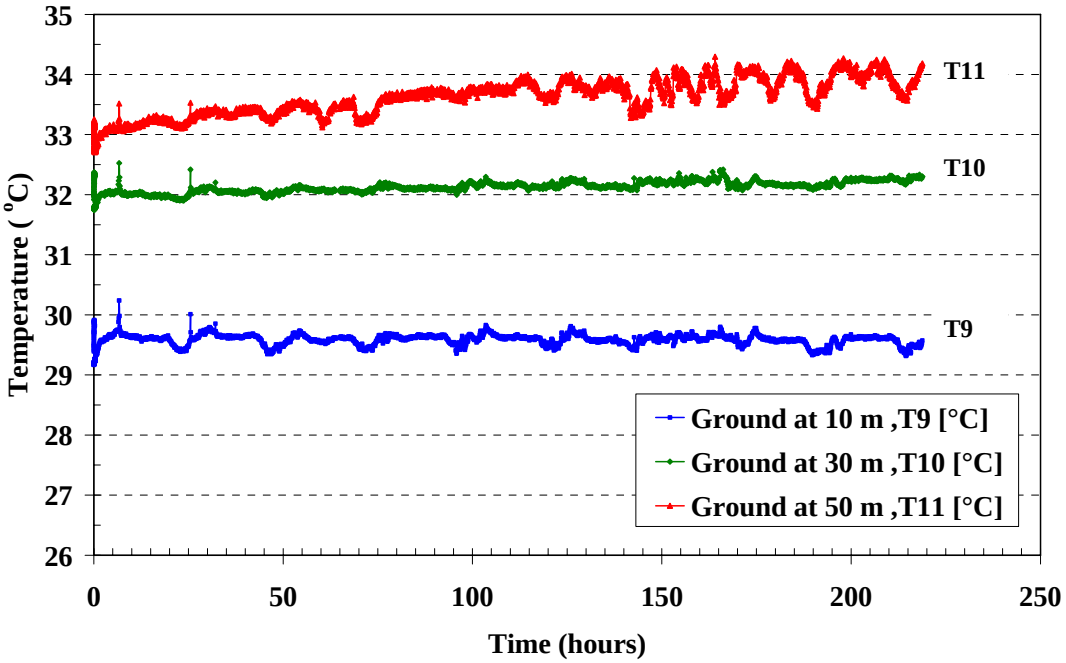
35
34
33
32
31
30
29
28
27
26
Temperature (°C)
0
50
100
150
200
250
Time (hours)
T11
T10
T9
Ground at 10 m ,T9 [°C]
Ground at 30 m ,T10 [°C]
Ground at 50 m ,T11 [°C]

Fig. 6

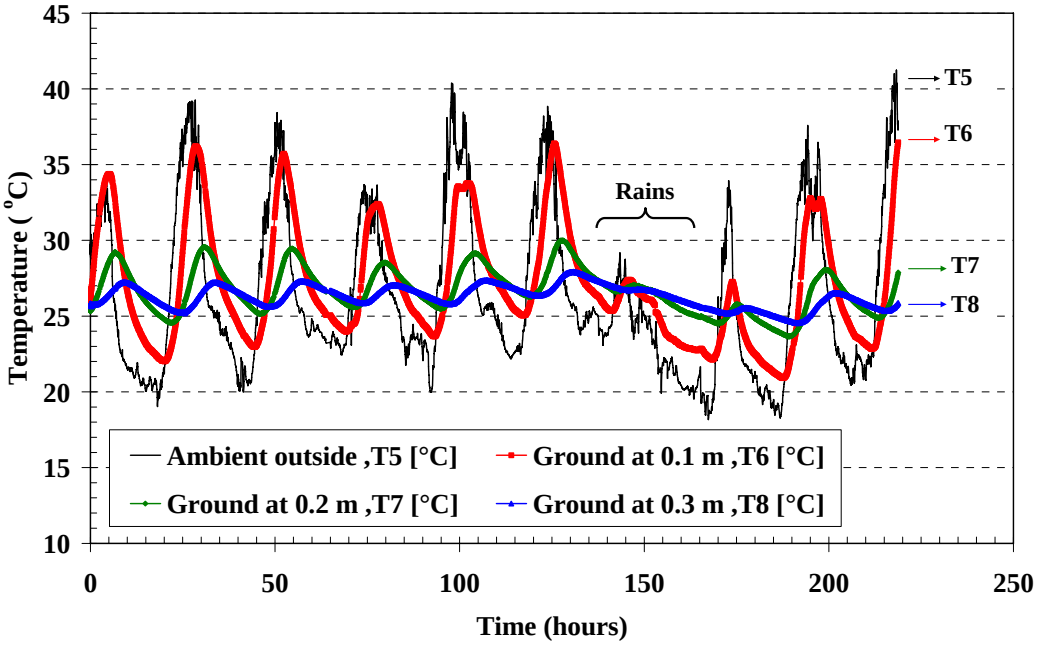
45
40
35
30
25
20
15
10
Temperature (°C)
0
50
100
150
200
250
Time (hours)
Rains
T5
T6
T7
T8
Ambient outside ,T5 [°C]
Ground at 0.1 m ,T6 [°C]
Ground at 0.2 m ,T7 [°C]
Ground at 0.3 m ,T8 [°C]

Fig. 7

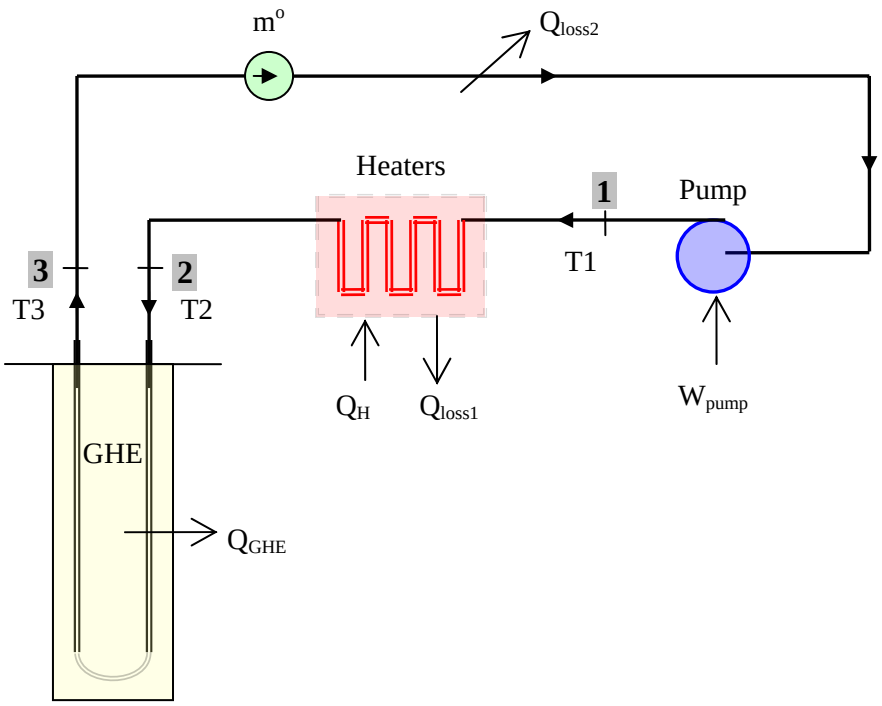

Fig. 8

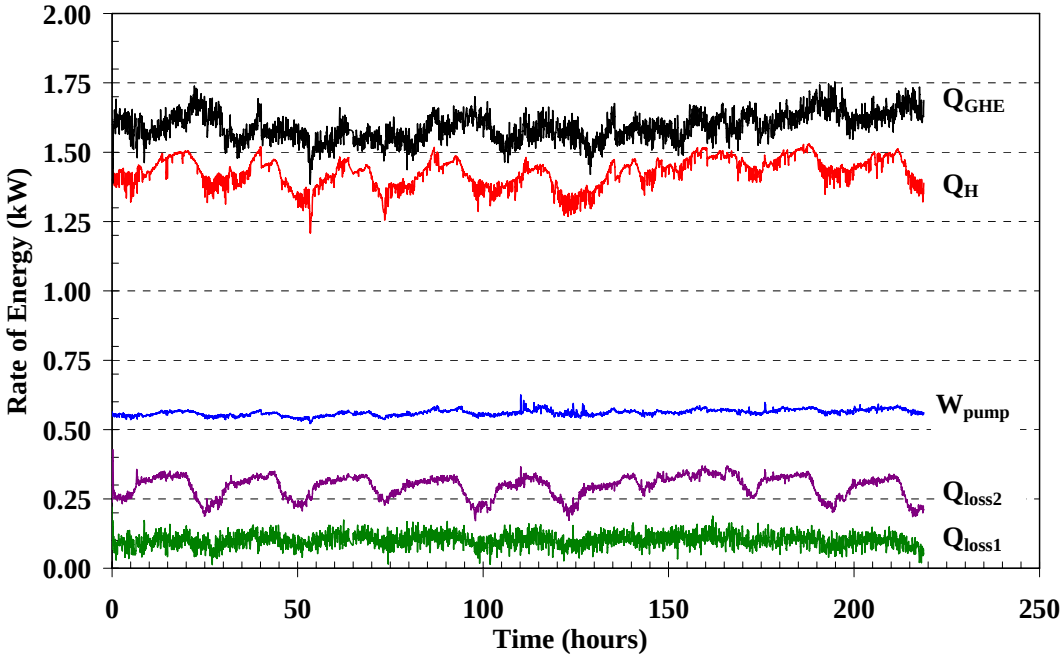
2.00
1.75
1.50
1.25
1.00
0.75
0.50
0.25
0.00
Rate of Energy (kW)
0
50
100
150
200
250
Time (hours)
Q_{GHE}
Q_H
W_{pump}
Q_{loss2}
Q_{loss1}

Fig. 9

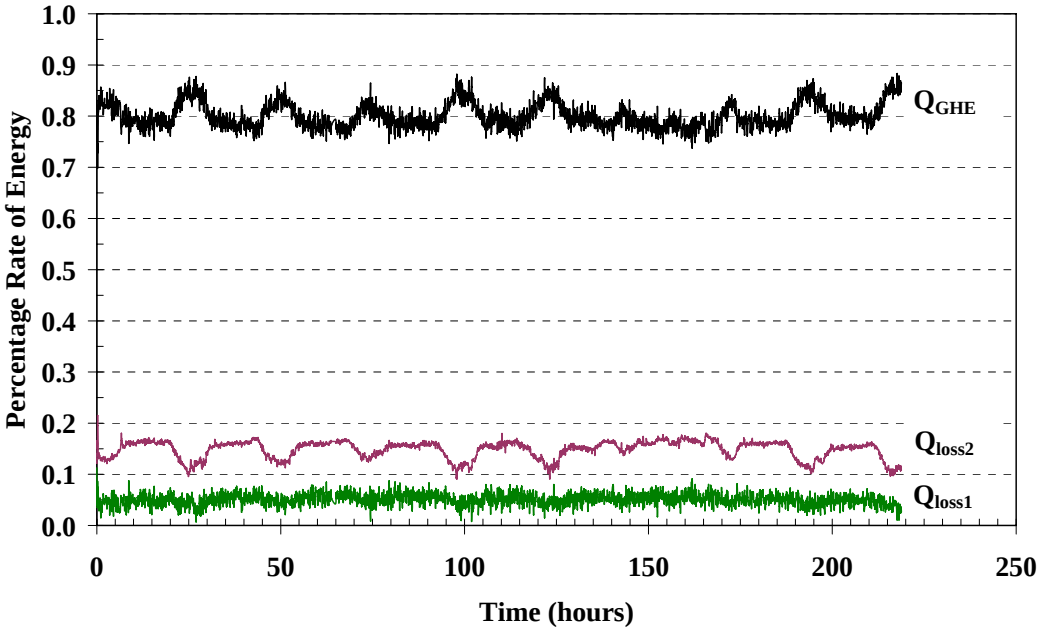
1.0
0.9
0.8
0.7
0.6
0.5
0.4
0.3
0.2
0.1
0.0
Percentage Rate of Energy
0
50
100
150
200
250
Time (hours)
Q_{GHE}
Q_{loss2}
Q_{loss1}

Fig. 10

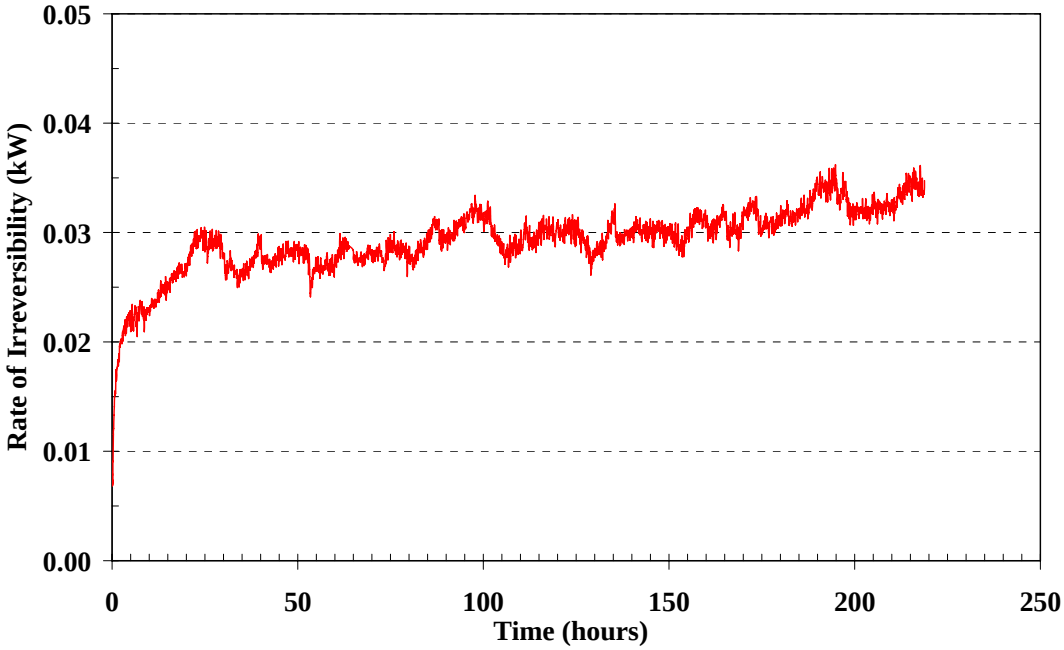
0.05
0.04
0.03
0.02
0.01
0.00
Rate of Irreversibility (kW)
0
50
100
150
200
250
Time (hours)

Fig. 11

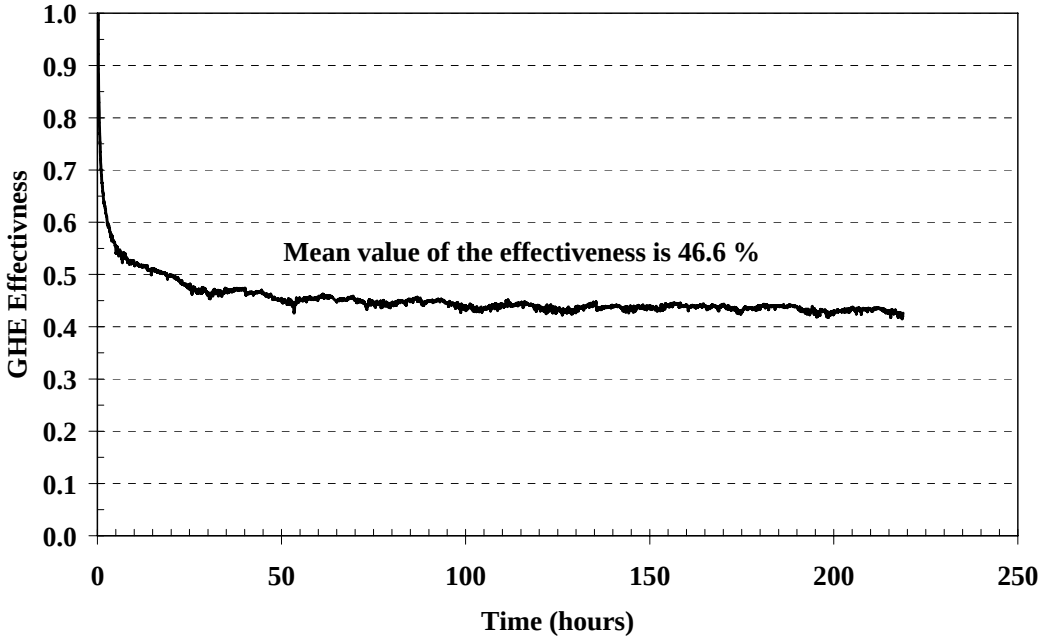
1.0
0.9
0.8
0.7
0.6
0.5
0.4
0.3
0.2
0.1
0.0
GHE Effectivness
Mean value of the effectiveness is 46.6 %
0
50
100
150
200
250
Time (hours)